

configuration interaction in transitions of the $2p$ - ns and $2p$ - nd type. This effect is not large, as was already noted by Hartree, Hartree, and Swirles,²⁴ but quantitative measures for transition probabilities may prove useful. These results are shown in Table IX, which presents dipole integrals from the $2p^3(^2P)$ term of OII to various upper states for the Hartree-Hartree-Swirles 2P wave functions with configuration interaction and without configuration interaction, respectively. The available AHF values¹⁷ are included in the table for direct comparison. These latter results do not, of course, include any of the effects of superposition of configurations.

ACKNOWLEDGMENTS

The authors wish to acknowledge a number of discussions with Dr. Robert R. Johnston and Dr. Maurice Cohen, and the helpful suggestions they provided have been incorporated into this paper. Dr. Paul S. Kelly lent much assistance and unpublished material, and Rex Page assisted with the computer programming. The encouragement of Professor D. R. Bates is gratefully acknowledged. Part of this work was done while the authors were associated with Lockheed Palo Alto Research Laboratories.

Hyperfine Structure $^2D_{5/2}$ and $^4F_{9/2}$ States of Ag^{107} and Ag^{109}

ARTHUR G. BLACHMAN,* DONALD A. LANDMAN,† AND ALLEN LURIO

IBM Watson Laboratory, Columbia University, New York, New York

(Received 6 April 1966)

The hfs of the $(4d^95s^2)^2D_{5/2}$ and $(4d^95s5p)^4F_{9/2}$ metastable electronic states in Ag^{107} and Ag^{109} have been measured by the atomic-beam magnetic-resonance method. The results, including the hfs dipole interaction constants which have been corrected for second-order interactions with neighboring fine-structure levels, are as follows:

$$\begin{aligned} \Delta\nu(\text{Ag}^{109}; ^2D_{5/2}; F=3 \leftrightarrow F=2) &= 435.4750(15) \text{ Mc/sec,} \\ \Delta\nu(\text{Ag}^{107}; ^2D_{5/2}; F=3 \leftrightarrow F=2) &= 378.8453(3) \text{ Mc/sec,} \\ \Delta\nu(\text{Ag}^{109}; ^4F_{9/2}; F=5 \leftrightarrow F=4) &= 1841.1564(9) \text{ Mc/sec,} \\ \Delta\nu(\text{Ag}^{107}; ^4F_{9/2}; F=5 \leftrightarrow F=4) &= 1596.7506(6) \text{ Mc/sec,} \\ A(^2D_{5/2})^{109} &= -145.1584(5) \text{ Mc/sec,} \quad A(^2D_{5/2})^{107} = -126.2818(1) \text{ Mc/sec,} \\ A(^4F_{9/2})^{109} &= -368.214(9) \text{ Mc/sec,} \quad A(^4F_{9/2})^{107} = -319.339(5) \text{ Mc/sec.} \end{aligned}$$

The hfs anomaly for each of the two states is

$$^{107}\Delta^{109}(^2D_{5/2}) = 0.00012(1) \quad \text{and} \quad ^{107}\Delta^{109}(^4F_{9/2}) = -0.00298(3).$$

By comparing the anomaly in the $^2D_{5/2}$ state with that in the ground $^2S_{1/2}$ state, we have obtained the amount of s -state mixing into the $^2D_{5/2}$ state. The contribution to the hfs of the $^4F_{9/2}$ level from each of the individual valence electrons has been estimated. The observed anomaly in the $^4F_{9/2}$ state is in good agreement with the estimated s -electron contribution to the state.

I. INTRODUCTION

THIS is the first in a series of papers devoted to the study of the hfs of several excited metastable electronic levels of the naturally occurring isotopes of the group Ib elements, $\text{Cu}^{63,65}$, $\text{Ag}^{107,109}$, and Au^{197} .¹ The hfs measurements were made by the atomic-beam magnetic-resonance method. Each of the three elements has an $[nd^{10}, (n+1)s]^2S_{1/2}$ ground state and each possesses at least one metastable level arising from its $[nd^9, (n+1)s^2]$ configuration and a metastable $^4F_{9/2}$ level

arising from its $[nd^9, (n+1)s, (n+1)p]$ configuration. In this paper, we report on the measurements of the hfs separations of the $(4d^95s^2)^2D_{5/2}$ and $(4d^95s5p)^4F_{9/2}$ levels in Ag^{107} and Ag^{109} .

Precision hfs measurements on several levels of an atom are of interest because they frequently provide a good check on the consistency of the interpretations of the results on the individual states. These checks are facilitated by analyzing the various hfs measurements into the contributions from the individual valence electrons. This is the procedure we have followed and, as will be seen below, the results are entirely satisfactory.

II. APPARATUS

The apparatus used in this experiment was essentially the same as that described in detail by Lurio²

* Present location: IBM Research Center, Yorktown Heights, New York.

† Present location: New York University, University Heights, Bronx, New York.

¹ A. G. Blachman and A. Lurio, *Bull. Am. Phys. Soc.* **8**, 9 (1963); **8**, 351 (1963); D. A. Landman, A. G. Blachman, and A. Lurio, *Brookhaven Conference on Molecular and Atomic Resonance*, Uppsala, Sweden, 1964 (unpublished).

² A. Lurio, *Phys. Rev.* **126**, 1768 (1962).

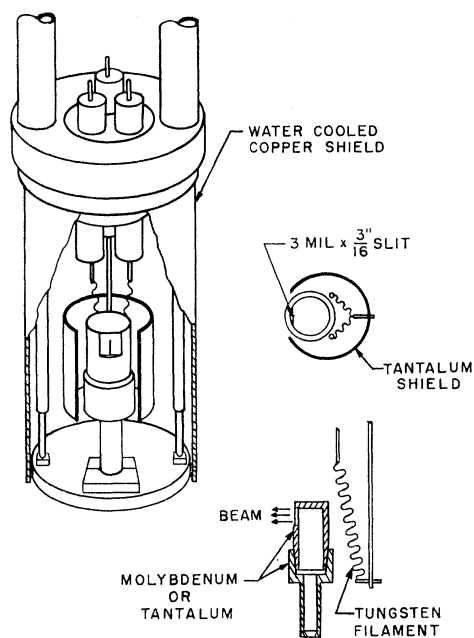


FIG. 1. Details of electron-bombardment source oven.

and hence will only briefly be discussed here. Except for the production and detection of the metastable Ag beam, the apparatus is a conventional atomic-beam magnetic-resonance device which was operated in the "flop-out" mode. The source of the Ag beam, shown in Fig. 1, consisted of a cylindrical Mo (or Ta) oven, which was electron bombardment heated to $\sim 1350^\circ\text{C}$. The Ag itself was placed in a graphite crucible (not shown in Fig. 1) inside the oven to prevent creep. The electron bombarder, for exciting the metastable states, is shown in Fig. 2, and was located immediately in front of the source oven. A fraction of the ground-state beam issuing from the oven and passing through the slit in the bombarder anode was excited by collisions with a vertically collimated electron beam, thereby populating the metastable states in the beam. After traversing the various magnetic fields and rf transition regions, the refocused portion of the beam was made to strike a Cs-coated surface. Collection and amplification of the electron current obtained from the resulting Auger de-excitation of the metastable atoms in the beam provided a detection system sensitive only to the metastable components of the beam.

The π and σ rf transition-inducing loops were constructed by folding over and by bending into an L shape, respectively, a Cu strip. The higher transition frequencies were monitored by beating, in a crystal diode, a small fraction of the oscillator signal with an appropriate combination of the 100 and 1000 Mc/sec signals produced by the Gr Type 1112 standard frequency multipliers. The beat-frequency signal was then fed, in turn, into a Beckman converter and counter. The 50th harmonic of the 100-kc/sec driving frequency

for the standard frequency multipliers was checked against the 5-Mc/sec WWV signal by means of a Blume "fade-canceling zero-beat indicator."³ The 100-kc/sec frequency was thereby kept accurate to within several parts in 10^7 .

III. THEORY

The hfs interaction Hamiltonian for an atom with nuclear spin $I = \frac{1}{2}$ can be written⁴

$$\mathcal{H}_{\text{hfs}} = [\sum_i T_e^{(1)}(i)] \cdot T_n^{(1)}, \quad (1)$$

where the tensor operators $T_e^{(1)}(i)$ and $T_n^{(1)}$ operate on the space of electron and nuclear coordinates, respectively, and the summation is over all the electrons. Denoting the nuclear state with $m_I = I$ by $|\beta II\rangle$ (where β denotes all other quantum numbers needed to specify the state completely), the nuclear magnetic dipole moment, μ_I , can be expressed in terms of $T_n^{(1)}$ by

$$\mu_I = \langle \beta II | T_n^{(1)} | \beta II \rangle.$$

In the nonrelativistic limit, the electron operator $T_e^{(1)}(i)$ can be written⁴

$$\begin{aligned} T_e^{(1)}(i) &= 2\mu_0 \{ \mathbf{l}_i - (\sqrt{10}) [C^{(2)}(\theta_i, \phi_i) \mathbf{s}_i]^{(1)} \} r_i^{-3}, & \text{for } l_i \neq 0; \\ &= (16\pi/3) \mu_0 \delta(\mathbf{r}_i) \mathbf{s}_i, & \text{for } l_i = 0. \end{aligned} \quad (2)$$

In this expression, μ_0 is the Bohr magneton, \mathbf{l}_i and \mathbf{s}_i are the orbital and spin angular momenta of the i th electron and $C_m^{(2)}(\theta_i, \phi_i)$ is related to the spherical harmonic $Y_{2m}(\theta_i, \phi_i)$ by $C_m^{(2)} = (4\pi/5)^{1/2} Y_{2m}$. The various relativistic and nuclear-size corrections to $T_e^{(1)}(i)$ are extensively discussed in the literature.⁵

A perturbation expansion for the hfs term energy can

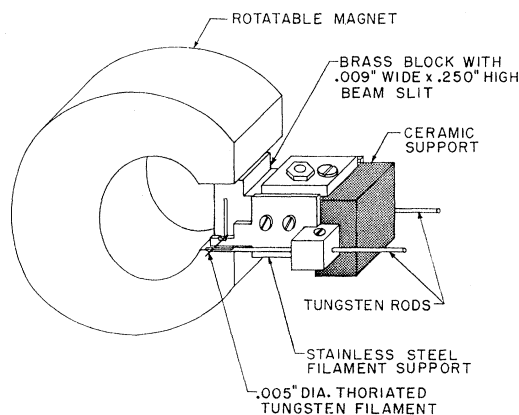


FIG. 2. Electron bombarder for the excitation of ground-state atoms to their metastable states.

³ R. J. Blume, *Rev. Sci. Instr.* **28**, 703 (1957).

⁴ C. Schwartz, *Phys. Rev.* **97**, 380 (1954); B. Judd, *Operator Techniques in Atomic Spectroscopy* (McGraw-Hill Book Company, Inc., New York, 1963), p. 84; R. E. Trees, *Phys. Rev.* **92**, 308 (1953).

⁵ See, e.g., H. Kopfermann, *Nuclear Moments* (Academic Press Inc., New York, 1958).

be obtained by using Eq. (1) together with a set of zero-order wave functions, $|\beta\frac{1}{2}\alpha J F m_F\rangle$, characterized by definite values of the nuclear ($I=\frac{1}{2}$), electronic (J), and total (F) angular momenta, the z component of $F(m_F)$, and any other nuclear (β) or electronic (α) quantum numbers needed to specify the state completely. We have, to second order,

$$W_{F,m_F} = W_F^{(1)} + W_F^{(2)} \\ = hA(\alpha J)\frac{1}{2}[F(F+1) - J(J+1) - \frac{3}{4}] + W_F^{(2)}, \quad (3)$$

where

$$A(\alpha J) = (1/IJ)\langle\alpha JJ|\sum_i T_e^{(1)}(i)|\alpha JJ\rangle \\ \times \langle\beta II|T_n^{(1)}|\beta II\rangle \quad (4)$$

is the magnetic dipole hfs interaction constant. The second-order term, $W_F^{(2)}$, will contribute significantly to the energy only when there are levels of total angular momentum F arising from hfs terms lying in the vicinity of the level of interest. Explicitly,

$$W_F^{(2)} = \sum'_{(\alpha'J')} |\langle\beta\frac{1}{2}\alpha J F m_F|\mathcal{H}_{\text{hfs}}|\beta\frac{1}{2}\alpha'J' F m_F\rangle|^2 [W(\alpha J) - W(\alpha'J')]^{-1} \\ = \sum'_{(\alpha'J')} \left\{ \begin{matrix} F & \frac{1}{2} & J' \\ 1 & J & \frac{1}{2} \end{matrix} \right\}^2 \langle\beta\frac{1}{2}\|T_n^{(1)}\|\beta\frac{1}{2}\rangle^2 \langle\alpha J|\sum_i T_e^{(1)}(i)|\alpha'J'\rangle^2 [W(\alpha J) - W(\alpha'J')]^{-1}, \quad (5)$$

where $[W(\alpha J) - W(\alpha'J')]$ is the fine-structure separation and the prime on the summation means that $\alpha'J' \neq \alpha J$. If the couplings of the relevant electronic states $|\alpha J\rangle$ are known, we can, by using Eq. (2), determine the contributions to the hfs from the individual valence electrons separately.

In the presence of a weak external magnetic field \mathbf{H} (which we take to define the z direction), the energy levels must be modified so as to include the magnetic interaction energy

$$\mathcal{H}_{\text{magnetic}} = \mu_0 g_J \mathbf{J} \cdot \mathbf{H} + \mu_0 g_I \mathbf{I} \cdot \mathbf{H} = \mu_0 H (g_J J_z + g_I I_z). \quad (6)$$

We assume here that J is a good quantum number. Treating $\mathcal{H}_{\text{magnetic}}$ as a perturbation, the change in the energy of the levels F, m_F correct to third order is

$$(W_{F,m_F})_{\text{magnetic}} = \mu_0 g_F H m_F + \left[\frac{\alpha^2}{W(\beta I \alpha J; F) - W(\beta I \alpha J; F+1)} + \frac{\beta^2}{W(\beta I \alpha J; F) - W(\beta I \alpha J; F-1)} \right] [\mu_0 H (g_J - g_I)]^2 \\ + \left\{ \frac{\alpha^2 (g_{F+1} - g_F)}{[W(\beta I \alpha J; F) - W(\beta I \alpha J; F+1)]^2} + \frac{\beta^2 (g_{F-1} - g_F)}{[W(\beta I \alpha J; F) - W(\beta I \alpha J; F-1)]^2} \right\} (\mu_0 H)^3 (g_J - g_I)^2 m_F, \quad (7)$$

where

$$\alpha^2 (F-1) = \beta^2 (F) = \frac{(F-I+J)(F+I-J)(I+J+1+F)(I+J+1-F)(F^2 - m^2)}{4F^2(2F-1)(2F+1)},$$

and

$$g_F = g_J \frac{F(F+1) + J(J+1) - I(I+1)}{2F(F+1)} + g_I \frac{F(F+1) + I(I+1) - J(J+1)}{2F(F+1)}.$$

IV. EXPERIMENTAL PROCEDURE AND RESULTS

A. Identification of the States

A graph of the Ag beam intensity, normalized to unit electron-bombarder current, as a function of the electron-bombarder voltage is shown in Fig. 3. The two peaks, occurring at ~ 6 V and ~ 11 V, indicate the presence of (at least) two metastable states and, as explained below, correspond to the production of the $(4d^9 5s^2)^2 D_{5/2}$ and $(4d^9 5s 5p)^4 F_{9/2}$ states, respectively.

Those Ag levels which might be metastable can be determined from a knowledge of the selection rules for electric-dipole transitions⁶ and consideration of the Ag

energy-level diagram⁷ shown in Fig. 4. The lowest possibly metastable levels are the $(4d^9 5s^2)^2 D_{5/2}$ level and any of the quartet levels arising from the $(4d^9 5s 5p)$ configuration.

Since $I = \frac{1}{2}$ for the two Ag isotopes, Ag^{107} and Ag^{109} , each fine-structure level splits into two hfs levels characterized by $F = J \pm \frac{1}{2}$. In a very small magnetic field, each hfs level splits into $2F+1$ sublevels. The ratio of the (degenerate) splitting $(\Delta E)_F \equiv |E(F, m) - E(F, m \pm 1)|$ for each fine-structure level is given by

$$\frac{(\Delta E)_{J+1/2}}{(\Delta E)_{J-1/2}} \approx \frac{J}{J+1}, \quad (8)$$

⁶ See, e.g., E. U. Condon and G. H. Shortley, *The Theory of Atomic Spectra* (Cambridge University Press, New York, 1935).

⁷ C. E. Moore, Natl. Bur. Std. U. S. Circ. No. 467 (1958).

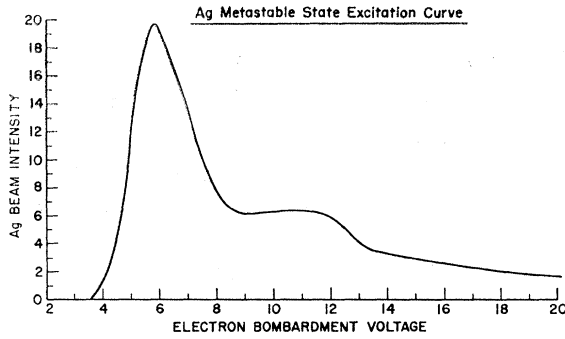


FIG. 3. Intensity of the metastable-state atomic beam as a function of bombarder voltage. The curve has been corrected for the variation in bombarder current with bombarder voltage.

neglecting terms of order g_I/g_J . It was observed that four transitions could be induced in the beam at weak magnetic fields. By comparing the ratios of these Zeeman transition frequencies with the ratios predicted by Eq. (8) for each of the above-mentioned possibilities and taking into consideration the various excitation energies of these states, the assignments $(4d^95s^2)^2D_{5/2}$ and $(4d^95s5p)^4F_{9/2}$ for the lower and upper peaks, respectively, in Fig. 4 were made. [Note that since there is only one $J = \frac{9}{2}$ level arising from the configuration $(4d^95s5p)$, it is independent of coupling and hence the $L-S$ designation 4F is valid.] The fact that the other quartet levels arising from the $(4d^95s5p)$ configuration are not sufficiently long-lived to be detected is most likely due to the breakdown of $L-S$ coupling in the configuration. This results in a mixing of the doublet and quartet levels so that transitions to the $(4d^95s^2)^2D_{3/2,5/2}$ levels are allowed. The identification of the $^2D_{5/2}$ and the $^4F_{9/2}$ levels was corroborated by obtaining the g_F for each of the observed low-field $\Delta F = 0$ Zeeman transitions. This was done by measuring in the same magnetic field as the Ag transitions were observed, the frequency of the transitions between the Zeeman levels of the even ($I=0$) isotopes of Mg in its metastable $(3s3p)^3P_{2,1}$ states. At a given magnetic field both the 3P_2 and 3P_1 states of Mg contribute to the transition due to the very near coincidence of the corresponding electronic g_J values. We have therefore

$$g_F(\text{Ag}) \approx [(\Delta\nu)_{F,\text{Ag}}/(\Delta\nu)_{\text{Mg}}]g_J(\text{Mg}), \quad (9)$$

in which $g_J(\text{Mg})$ is taken to be the mean of the electronic g factors of the two states and $(\Delta\nu)_{F,\text{Ag}}$ and $(\Delta\nu)_{\text{Mg}}$ are the observed transition frequencies in Ag and Mg, respectively. A theoretical calculation of $g_J(\text{Mg}; ^3P_2)$ and $g_J(\text{Mg}; ^3P_1)$ in which estimates of the relativistic and diamagnetic corrections⁸ were made gives $g_J(\text{Mg}) = 1.50114$. The results of a series of measurements to determine $g_J(\text{Ag}; ^4F_{9/2})$ are shown in Table I (runs 1-4). When the subsequent high-field

⁸ A. Abragam and J. H. Van Vleck, Phys. Rev. 92, 1448 (1953).

TABLE I. Experimental data and results for $g_J(\text{Ag}; ^4F_{9/2})$. (All frequency units are Mc/sec.)

Run	$\Delta\nu[(F,m) \leftrightarrow (F',m')]]$	$\Delta\nu[(^3P_{2,1,m} \leftrightarrow (^3P_{2,1,m \pm 1})]_{\text{Mg}}$	$g_J(\text{Ag}; ^4F_{9/2})$
1	$(4,m) \leftrightarrow (4, m \pm 1) = 9.663(10)$	9.902(10)	1.332
2	$(5,m) \leftrightarrow (5, m \pm 1) = 7.905(10)$	9.901(10)	1.332
3	$(4,m) \leftrightarrow (4, m \pm 1) = 4.251(10)$	4.332(10)	1.339
4	$(5,m) \leftrightarrow (5, m \pm 1) = 3.479(10)$	4.332(10)	1.339
5	$(5, -2) \leftrightarrow (5, -3) = 241.55(4)$	299.09(4)	1.3328
6	$(5, -1) \leftrightarrow (5, -2) = 241.28(4)$	299.09(4)	1.3345
7	$(5,0) \leftrightarrow (5, -1) = 240.85(4)$	299.09(4)	1.3355
8	$(5,1) \leftrightarrow (5,0) = 240.02(4)$	299.09(4)	1.3349
9	$(5,2) \leftrightarrow (5,1) = 239.21(4)$	299.09(4)	1.3347
10	$(5,3) \leftrightarrow (5,2) = 238.37(4)$	299.09(4)	1.3347
11	$(5,4) \leftrightarrow (5,3) = 237.25(4)$	299.09(4)	1.3334

measurements are included (runs 5-11), we get

$$g_J(\text{Ag}; ^4F_{9/2}) = 1.334(1), \quad (10)$$

a result which is in excellent agreement with the predicted value of 1.334. This theoretical value is expected to be quite reliable since it is independent of the electron coupling except for configuration interaction effects which are second order in the mixing coefficients.

B. The hfs Measurements

The hfs of the $^2D_{5/2}$ and $^4F_{9/2}$ levels is shown schematically as a function of an externally applied mag-

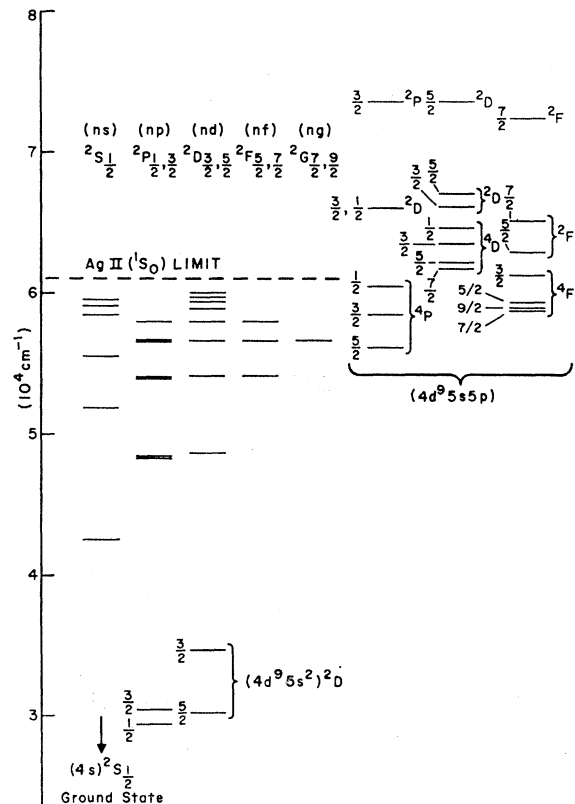


FIG. 4. Energy-level diagram of silver.

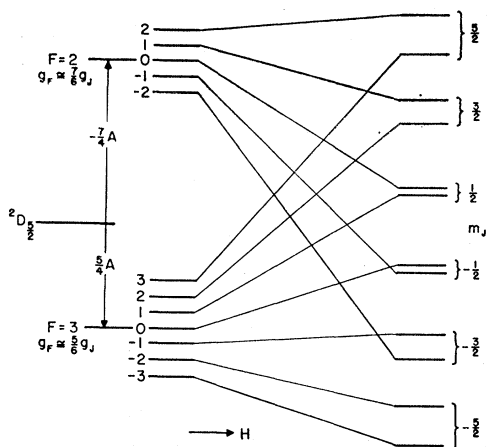


FIG. 5. A schematic plot of the magnetic field dependence of the hfs levels of the ${}^2D_{5/2}$ state.

netic field in Figs. 5 and 6, respectively. The inversion of the F levels for each fine-structure level is due to the fact that $\mu_I < 0$ for both isotopes.

The zero-field separations were obtained as follows. Using enriched Ag^{109} , we followed the Zeeman transitions within a given F level up in magnetic field until they were completely resolved (see Fig. 7). Equation (7)

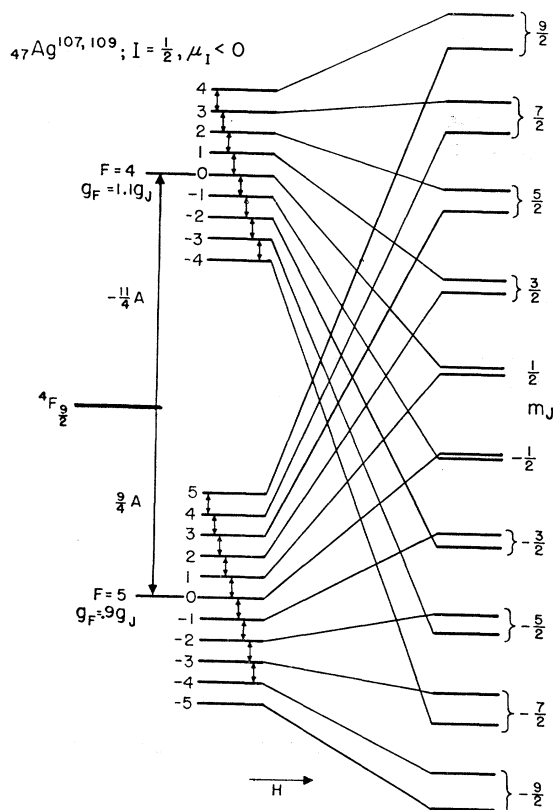


FIG. 6. A schematic plot of the magnetic-field dependence of the hfs levels of the ${}^4F_{9/2}$ state.

TABLE II. Experimental hfs data and results for $\text{Ag}^{107,109}$. (All frequency units are Mc/sec.)

Iso-	State	tope	F	$\Delta\nu[(F,0) \leftrightarrow (F-1,0)]$	$\mu_0 H$	$\Delta\nu[F \leftrightarrow (F-1)]$
${}^2D_{5/2}$	109	3		435.4752	0.448	435.4749
				435.4739	0.452	435.4736
				435.4758	0.454	435.4757
				435.4760	0.450	435.4757
${}^2D_{5/2}$	107	3		378.8456	0.473	378.8452
				378.8457	0.470	378.8453
				378.8458	0.468	378.8454
${}^4F_{9/2}$	109	5		1841.1569	1.20	1841.1562
				1841.1576	1.14	1841.1570
				1841.1569	1.43	1841.1560
${}^4F_{9/2}$	107	5		1596.7519	1.67	1596.7504
				1596.7513	1.25	1596.7504
				1596.7525	1.74	1596.7509

then relates the frequency of these resolved lines to the Ag^{109} zero-field hfs. With the estimates thereby obtained, a search for the $\Delta\nu[F, m] \leftrightarrow (F-1, m')$ σ - and π -transitions at very low magnetic field was made. When these were located, a series of precision measurements was made on the $\Delta\nu[(F,0) \leftrightarrow (F-1,0)]$ σ transitions (since they are field-independent to first order) in as low a field as possible for which the individual σ transitions were still clearly resolved. The results are given in Table II. A typical resonance curve is shown in Fig. 8. The signal to noise ratio $\sim 28:1$. Since the nuclear-magnetic dipole-moment ratio,

$$\mu^{107}/\mu^{109} = 0.86985(1),$$

had previously been measured,⁹ the corresponding transitions $\Delta\nu^{107}(F \leftrightarrow F-1)$ in Ag^{107} could be estimated

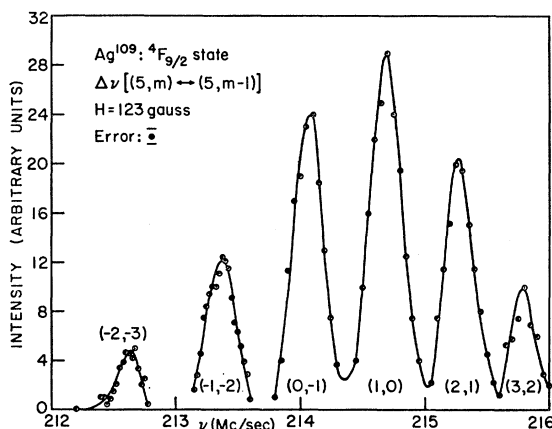


FIG. 7. $\Delta F=0, \Delta m_F = \pm 1$ transitions in the ${}^4F_{9/2}$ state of Ag^{109} . The splitting between the lines is used to estimate the zero-field hfs separation.

⁹ P. B. Sogo and C. D. Jeffries, Phys. Rev. **93**, 174 (1954); E. Brun, J. Oeser, H. H. Staub, and C. G. Telschow, *ibid.* **93**, 172 (1954).

by means of the relation

$$\Delta\nu^{107}(F \leftrightarrow F-1) = (\mu^{107}/\mu^{109})\Delta\nu^{109}(F \leftrightarrow F-1). \quad (11)$$

Using natural Ag in the beam, the $\Delta\nu^{107}[(F,0) \leftrightarrow (F-1,0)]\sigma$ transitions were easily found and measured in the manner described above (see Table II). After making the small, field-dependent corrections for each line, we obtain the following results for the hfs separations:

$$\begin{aligned} \Delta\nu(\text{Ag}^{109}; {}^2D_{5/2}; F=3 \leftrightarrow F=2) &= 435.4749(15) \text{ Mc/sec}, \\ \Delta\nu(\text{Ag}^{109}; {}^4F_{9/2}; F=5 \leftrightarrow F=4) &= 1841.1564(9) \text{ Mc/sec}, \\ \Delta\nu(\text{Ag}^{107}; {}^2D_{5/2}; F=3 \leftrightarrow F=2) &= 378.8453(3) \text{ Mc/sec}, \\ \Delta\nu(\text{Ag}^{107}; {}^4F_{9/2}; F=5 \leftrightarrow F=4) &= 1596.7506(6) \text{ Mc/sec}. \end{aligned} \quad (12)$$

The error quoted in each of the above results is three times the standard deviation of the mean of all determinations of that quantity so as to allow for a possible unfavorable accumulation of errors in the relatively small number of runs made.

From the transit time of the Ag beam down the apparatus, a lower limit of ~ 1 msec is obtained for the lifetimes of both the ${}^2D_{5/2}$ and ${}^4F_{9/2}$ levels.

V. DISCUSSION OF RESULTS

A. Wave Functions

In order to analyze the results presented above it is necessary to know the coupling of the electrons in the

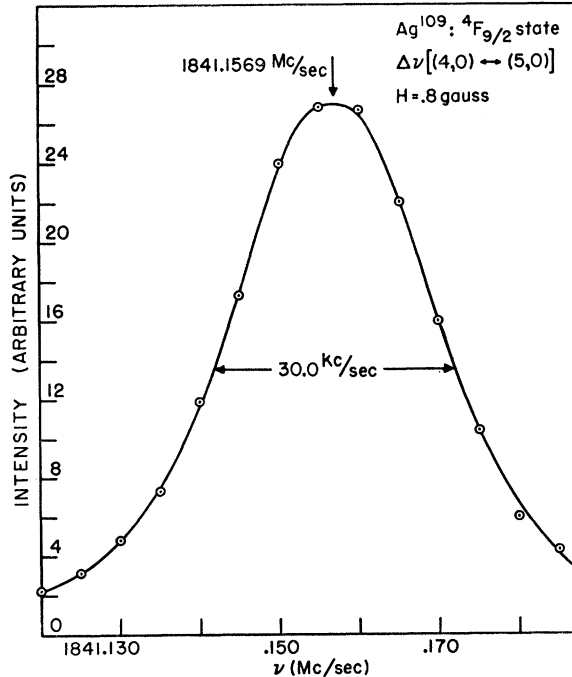


FIG. 8. A typical experimental curve used in determining the $F=5$ to $F=4$ zero-field hfs separation in the ${}^4F_{9/2}$ state of Ag^{109} . The line has the expected natural width.

configurations (core)($4d^95s^2$) and (core)($4d^95s5p$) which give rise to the ${}^2D_{5/2}$ and ${}^4F_{9/2}$ levels, respectively. We will initially treat the problem in each case from a single configuration point of view. Within each configuration, however, we will estimate the second-order contributions to the hfs from nearby fine-structure levels since these are the ones which lie closest in energy and can give contributions to within the precision of the measurements. It will be seen below that this approach is particularly consistent with the results for the ${}^2D_{5/2}$ level, but, because of the much greater complexity of the ($4d^95s5p$) configuration, the situation is not as certain for the case of the ${}^4F_{9/2}$ level.

Since the ($4d^95s^2$) ${}^2D_{3/2}$, ${}^2D_{5/2}$, and ($4d^95s5p$) ${}^4F_{9/2}$ levels are the only ones with those J values in their respective configurations, their wave functions are independent of coupling to the approximation we are considering. The other wave functions of a given J value in the ($4d^95s5p$) configuration can be described as orthogonal superpositions of all the wave functions of that J value obtained from any complete set for the configuration. Unfortunately, the fact that some of these levels have not yet been observed, combined with the general complexity of the spectrum, renders a detailed analysis of the mixing of these levels prohibitively difficult. However, the observed groupings and orderings of the levels (see Fig. 4) indicate that the coupling is approximately L - S . In particular, $({}^4D-{}^4F)/({}^4F-{}^4P)=2.0$ (where the energies of the terms are taken to be the centers of gravity of the component levels), in fair agreement with the predicted value of 1.8 for pure L - S coupling.¹⁰ Since consideration of these levels arises only in the calculation of the very small second-order corrections to the dipole coupling constants, we will therefore assume that the corresponding wave functions can be adequately described by L - S coupling. (In this connection, it should be noted that the indication of mixing mentioned in Sec. IV as arising from the failure to observe any of the other quartet levels in the beam does not contradict this assumption since only a very small mixing of the doublet levels is enough to reduce the lifetime sufficiently.)

B. Calculation of the Magnetic Dipole hfs Interaction Constants

From Eq. (3), the zero-field hfs separations for either isotope can be written

$$h\Delta\nu({}^2D_{5/2}) = |W(F=3) - W(F=2)| = -3hA({}^2D_{5/2}) + W_2^{(2)}({}^2D_{5/2}) - W_3^{(2)}({}^2D_{5/2}), \quad (13)$$

and

$$h\Delta\nu({}^4F_{9/2}) = |W(F=5) - W(F=4)| = -5hA({}^4F_{9/2}) + W_4^{(2)}({}^4F_{9/2}) - W_5^{(2)}({}^4F_{9/2}). \quad (14)$$

¹⁰ G. Racah, Phys. Rev. **62**, 523 (1942); M. Elbel, Ann. Physik **13**, 217 (1964).

With the measured values given above, and neglecting the second-order terms, we get

$$\begin{aligned} A({}^2D_{5/2}) &= -145.1584(5) \text{ Mc/sec} \quad (\text{for } \text{Ag}^{109}), \\ &= -126.2818(1) \text{ Mc/sec} \quad (\text{for } \text{Ag}^{107}), \end{aligned}$$

and

$$\begin{aligned} A({}^4F_{9/2}) &= -368.2313(2) \text{ Mc/sec} \quad (\text{for } \text{Ag}^{109}), \\ &= -319.3501(1) \text{ Mc/sec} \quad (\text{for } \text{Ag}^{107}). \end{aligned}$$

By evaluating the matrix elements in Eqs. (4) and (5), the various A constants and second-order energy terms can be expressed in terms of contributions from the individual valence electrons. For the A constants, we obtain

$$A({}^2D_{5/2}) = a(d_{5/2})_D, \quad (15)$$

$$A({}^4F_{9/2}) = \frac{1}{3}a(s) + \frac{1}{3}a(p_{3/2}) + (5/9)a(d_{5/2})_F,$$

where the single-electron magnetic dipole interaction constants $a(l_j)$ are defined by

$$\begin{aligned} a(l_j) &\equiv (1/Ij) \langle \beta II | T_n^{(1)} | \beta II \rangle \langle \frac{1}{2} l j j | T_e^{(1)} | \frac{1}{2} l j j \rangle, \\ &= (16/3) \pi \mu_0 (\mu_I/I) |\psi(0)|^2 F_r(0, \frac{1}{2}, Z_i) (1-\delta)(1-\epsilon), \end{aligned}$$

for $l=0$, (16)

$$= 2\mu_0 \frac{\mu_I l(l+1)}{I j(j+1)} \langle r^{-3} \rangle F_r(l, j, Z_i) (1-\delta)(1-\epsilon),$$

for $l \neq 0$.

In these expressions, $\psi(0)$ is the electronic wave function at the nucleus, F_r is a relativistic correction factor, Z_i is the effective nuclear charge and the factors $(1-\delta)$ and $(1-\epsilon)$ are corrections for the distribution of nuclear charge and current, respectively, throughout the volume of the nucleus. The D and F subscripts on the $a(d_{5/2})$ coupling constants serve merely to distinguish the relevant fine-structure level. The matrix elements arising in the calculation of the various terms contributing to $W_F^{(2)}$ are given in Appendix A.

The procedure for estimating the single-electron coupling constants is as follows. A value of $a(d_{5/2})_D$ for each isotope is obtained immediately by ignoring the small second-order energy corrections in $A({}^2D_{5/2})$. When these values are substituted into Eq. (5), the second-order energy corrections for the ${}^2D_{5/2}$ level are found not to be significant to within the accuracy of the experimental results. Correspondingly, for the ${}^4F_{9/2}$ level, we have

$$\begin{aligned} \frac{1}{3}a(s) + \frac{1}{3}a(p_{3/2}) + (5/9)a(d_{5/2})_F \\ \approx -368.2 \text{ Mc/sec} \quad (\text{for } \text{Ag}^{109}), \\ \approx -319.4 \text{ Mc/sec} \quad (\text{for } \text{Ag}^{107}). \end{aligned} \quad (17)$$

Since $a(s) > a(p_{3/2})$ and $a(d_{5/2})_F$, the latter two quantities will be estimated from the measured hfs of the $(4d^{10}5p)^2P_{1/2}$ and ${}^2P_{3/2}$ levels and from the $(4d^95s)^2D_{5/2}$ level, respectively, and then $a(s)$ will be deduced. We

have

$$\begin{aligned} a(p_{3/2}) &\approx -35 \text{ Mc/sec} \\ &\approx -29 \text{ Mc/sec} \\ \text{and } a(d_{5/2})_F &\approx -145 \text{ Mc/sec} \quad (\text{for } \text{Ag}^{109}) \\ &\approx -126 \text{ Mc/sec} \quad (\text{for } \text{Ag}^{107}) \end{aligned} \quad (18)$$

resulting in the values

$$\begin{aligned} a(s) &= -2498(195) \text{ Mc/sec} \quad (\text{for } \text{Ag}^{109}) \\ &= -2150(160) \text{ Mc/sec} \quad (\text{for } \text{Ag}^{107}). \end{aligned} \quad (19)$$

[The uncertainties in $a(s)$ were estimated by observing that the ground-state hfs gives

$$\begin{aligned} a(s) &= -1976.94(4) \text{ Mc/sec} \quad (\text{for } \text{Ag}^{109}) \\ &= -1712.56(4) \text{ Mc/sec} \quad (\text{for } \text{Ag}^{107}). \end{aligned}$$

Since these values are $\sim 20\%$ larger than the results of Eq. (19), an error of 25% was assumed for the above values of $a(p_{3/2})$ and $a(d_{5/2})_F$.]

Evaluating the second-order energy corrections, we obtain

$$\begin{aligned} A({}^2D_{5/2}) &= -145.1584(5) \text{ Mc/sec} \quad \text{and} \quad A({}^4F_{9/2}) \\ &= -126.2818(1) \text{ Mc/sec} \\ &= -368.214(9) \text{ Mc/sec} \quad (\text{for } \text{Ag}^{109}) \\ &= -319.339(5) \text{ Mc/sec} \quad (\text{for } \text{Ag}^{107}), \end{aligned} \quad (20)$$

where an uncertainty of 50% was assumed for $[W_5^{(2)}({}^4F_{9/2}) - W_4^{(2)}({}^4F_{9/2})]$ because of the uncertainty in the electron coupling.

The value of $A({}^2D_{5/2})$ can be predicted by using (i) the value of $\langle r^{-3} \rangle$ for a d electron obtained from the fine-structure splitting, $W({}^2D_{3/2}) - W({}^2D_{5/2})$:

$$\langle r^{-3} \rangle_d = \frac{\zeta_{5d}}{2\mu_0^2 Z_i H_r(2, Z_i)} = \frac{\frac{2}{3} [W({}^2D_{3/2}) - W({}^2D_{5/2})]}{2\mu_0^2 Z_i H(2, Z_i)}, \quad (21)$$

in which ζ_{5d} is the spin-orbit radial integral for a d electron and $H_r(l, Z_i)$ is a relativistic correction factor; and (ii) the measured values of the nuclear magnetic dipole moments (including the diamagnetic correction) for the two isotopes:

$$\begin{aligned} \mu_I &= -0.130538 \text{ nm} \quad (\text{for } \text{Ag}^{109}), \\ &= -0.113548 \text{ nm} \quad (\text{for } \text{Ag}^{107}). \end{aligned}$$

Taking $Z_i = Z - 11^{(11)} = 36$, we obtain the values

$$\begin{aligned} A({}^2D_{5/2}) &= -146 \text{ Mc/sec} \quad (\text{for } \text{Ag}^{109}), \\ &= -127 \text{ Mc/sec} \quad (\text{for } \text{Ag}^{107}), \end{aligned} \quad (22)$$

in excellent agreement with the measured results.

C. The hfs Anomaly

The hfs anomaly is defined by the equation ${}^{107}\Delta^{109} \equiv (A^{107}g_I^{109}/A^{109}g_I^{107}) - 1$. The experimental value of the

¹¹ See Ref. 5, p. 131.

anomaly for each fine structure level is

$$\begin{aligned} {}^{107}\Delta^{109}({}^2D_{5/2}) &= 0.00012(1), \\ {}^{107}\Delta^{109}({}^4F_{9/2}) &= -0.00298(3), \end{aligned} \quad (23)$$

where the g_I ratio $g_I^{109}/g_I^{107} = 1.14962(1)$ has been taken from nuclear induction measurements.⁹ From previous hfs measurements in the $(4d^{10}5s)^2S_{1/2}$ ground state¹² we have the value ${}^{107}\Delta^{109}({}^2S_{1/2}) = -0.00412(6)$.

As is well known, the hfs anomaly can be explained by treating the nucleus as an extended charge and current distribution, differing from isotope to isotope. In such a model, the point interactions must be replaced by suitable averages over the nuclear current distribution and the electronic wave functions must be modified to take into account the changed nuclear potential. The results of these changes will be most pronounced in configurations containing unpaired s electrons (and to a lesser extent in configurations containing unpaired $p_{1/2}$ electrons in heavy atoms) because of their finite charge densities at the nucleus. Accordingly, we will assume that the relations

$$\frac{a(p_{3/2})^{109}}{a(p_{3/2})^{107}} = \frac{a(d_{5/2})^{109}}{a(d_{5/2})^{107}} = \frac{g_I^{109}}{g_I^{107}}$$

are valid.

The fact that ${}^{107}\Delta^{109}({}^2D_{5/2})$ does not vanish can be explained by assuming a small mixing into the wave function for the ${}^2D_{5/2}$ level by configurations having unpaired s electrons. If we assume such a mixing due to configurations such as $(4d^95sns)$, then from Appendix B we have

$$A({}^2D_{5/2}) = a(4d_{5/2}) - a_s.$$

With this equation and the equation defining the anomaly we can derive the result

$${}^{107}\Delta^{109} = - (a_s^{109}/A^{109}) {}^{107}\Delta_s^{109} \simeq - (a_s^{107}/A^{107}) {}^{107}\Delta_s^{109}.$$

The quantity

$${}^{107}\Delta_s^{109} \equiv \frac{a(ns)^{107} g^{109}}{a(ns)^{109} g^{107}} - 1$$

is taken to be the same for all s electron states in the atom and is equal to ${}^{107}\Delta^{109}({}^2S_{1/2})$. Comparison of this result with the experimental results enables one to obtain $a_s = (0.029A({}^2D_{5/2}))$. The small size of a_s compared to $a(d_{5/2})$ is consistent with the excellent agreement of the calculated and experimental values of $a(d_{5/2})$ given in the previous section. It is also consistent with the magnitude and sign of the mixing calculated by Koster¹³ for the case of gallium.

¹² G. Wessel and H. Lew, Phys. Rev. **92**, 641 (1953).

¹³ G. F. Koster, Phys. Rev. **86**, 148 (1952).

For the $(d^9s^2)^4F_{9/2}$ level one would expect the hfs anomaly to arise from the s electron alone. Thus we expect [see Eq. (15)]

$$\begin{aligned} {}^{107}\Delta^{109}({}^4F_{9/2}) &= \frac{1}{9}[a(s)/A] {}^{107}\Delta^{109}({}^2S_{1/2}) \\ &\cong [2498/9(368)](-0.00412) \\ &= -0.0031. \end{aligned}$$

The close agreement between this result and the experimental value of ${}^{107}\Delta^{109}({}^4F_{9/2})$ is confirmation of our estimate of the $a(s)$ contribution to the ${}^4F_{9/2}$ hfs. In the present results we see that the hfs anomaly can be used as a probe to learn the s -electron contribution to an atomic state. In this regard it may prove more useful than its original use, i.e., to learn about nuclear structure.

APPENDIX A

The four $J = \frac{7}{2}$ L - S coupled wave functions for the $(4d^95s^2p)$ configuration can be written $|{}^4F_{7/2}\rangle$, $|{}^4D_{7/2}\rangle$,

$$c_1|[d^9s({}^3D)p]^2F_{7/2}\rangle + c_2|[d^9s({}^1D)p]^2F_{7/2}\rangle,$$

and

$$c_2|[d^9s({}^3D)p]^2F_{7/2}\rangle - c_1|[d^9s({}^1D)p]^2F_{7/2}\rangle,$$

where the two ${}^2F_{7/2}$ levels are written as linear combinations of the wave functions formed by using the $d^9s({}^1,{}^3D)$ parent system. The mixing coefficients c_1 and c_2 are functions of the appropriate electrostatic radial integrals.

The matrix elements needed for the evaluation of the second-order energy corrections for the ${}^4F_{9/2}$ level are

$$\begin{aligned} \langle {}^4F_{9/2} || T_e^{(1)} || {}^4F_{7/2} \rangle \\ = (1/\mu_I) (\frac{5}{2})^{1/2} [\frac{1}{3}a(s) - \frac{1}{6}a_p - (3/7)(a_d)_F], \end{aligned}$$

$$\begin{aligned} \langle {}^4F_{9/2} || T_e^{(1)} || {}^4D_{7/2} \rangle \\ = (1/\mu_I) \frac{1}{2} (15)^{1/2} [-\frac{3}{5}a_p + (5/7)(a_d)_F], \end{aligned}$$

$$\begin{aligned} \langle {}^4F_{9/2} || T_e^{(1)} || [d^9s({}^3D)p]^2F_{7/2} \rangle \\ = (1/\mu_I) (\frac{5}{8})^{1/2} [\frac{1}{2}a(s) - \frac{1}{5}a_p - (1/7)(a_d)_F], \end{aligned}$$

$$\begin{aligned} \langle {}^4F_{9/2} || T_e^{(1)} || [d^9s({}^1D)p]^2F_{7/2} \rangle \\ = (1/\mu_I) (\frac{5}{2})^{1/2} [\frac{1}{2}a(s) + (1/7)(a_d)_F], \end{aligned}$$

where we have defined $a_l \equiv 2\mu_0(\mu_I/I)\langle r^{-3} \rangle_l$ and we have neglected all relativity and nuclear size correction factors. In view of the magnitudes of $a(s)$, a_p , a_d , and the various energy separations $[W(\frac{9}{2}) - W(\alpha, \frac{7}{2})]$, only the ${}^4F_{7/2}$ level need be included in the sum over states in Eq. (5).

For the $(d^9s^2)^2D_{5/2,3/2}$ levels we have

$$\langle {}^2D_{5/2} || T_e^{(1)} || {}^2D_{3/2} \rangle = - (1/\mu_I) \frac{7}{16} (5/3)^{1/2} a(d_{5/2})_D.$$

APPENDIX B

In this Appendix we derive expressions for the effect on the magnetic-dipole hfs interaction constants of the ${}^2l_{\pm 1/2}$ states due to mixing of the (core)(ns)($n's$)($n''l$) electron configuration with the (core)(ns^2)($n''l$) electron configuration. The derived results are a generalization of the calculation by Koster¹³ who considered the case $l=1$. It should be noted that all the results remain valid if the ($n''l$) electron is replaced by a ($n''l$) hole.

We expand the states as follows:

$$|\gamma^2l_{\pm 1/2}, m\rangle = \alpha_0 |(ns^2)[{}^1S](n''l); {}^2l_{\pm 1/2}, m\rangle + \alpha_1 |(ns)(n's)[{}^3S](n''l); {}^2l_{\pm 1/2}, m\rangle + \alpha_2 |(ns)(n's)[{}^1S](n''l); {}^2l_{\pm 1/2}, m\rangle. \quad (\text{B1})$$

The wave functions on the right-hand side of Eq. (B1) are constructed by first coupling the two s electrons to form ${}^1, {}^3S$ states which are then coupled with the l electron to form the ${}^2l_{\pm 1/2}$ states. The coupling coefficients α_i ($i=0, 1, 2$) satisfy the normalization condition

$$\sum_{i=0}^2 \alpha_i^2 = 1.$$

Because the hfs Hamiltonian is a sum of single-electron operators, it is convenient to work with a set of jj coupled states. By means of the recoupling formulas¹⁴ it can be shown that

$$\begin{aligned} |(ns^2)[{}^1S](n''l); {}^2l_{\pm 1/2}, m\rangle &= |(ns_{1/2})^2[{}^0](n''l_{\pm 1/2}); l \pm 1/2, m\rangle, \\ |(ns)(n's)[{}^3S](n''l); {}^2l_{+1/2}, m\rangle &= \left[\frac{2l+3}{3(2l+1)} \right]^{1/2} |(ns_{1/2})(n's_{1/2})[{}^1](n''l_{+1/2}); l+1/2, m\rangle \\ &\quad - \left[\frac{4l}{3(2l+1)} \right]^{1/2} |(ns_{1/2})(n's_{1/2})[{}^1](n''l_{-1/2}); l+1/2, m\rangle, \quad (\text{B2}) \\ |(ns)(n's)[{}^3S](n''l); {}^2l_{-1/2}, m\rangle &= \left[\frac{4l+4}{3(2l+1)} \right]^{1/2} |(ns_{1/2})(n's_{1/2})[{}^1](n''l_{+1/2}); l-1/2, m\rangle \\ &\quad - \left[\frac{2l-1}{3(2l+1)} \right]^{1/2} |(ns_{1/2})(n's_{1/2})[{}^1](n''l_{-1/2}); l-1/2, m\rangle, \\ |(ns)(n's)[{}^1S](n''l); {}^2l_{\pm 1/2}, m\rangle &= |(ns_{1/2})(n's_{1/2})[{}^0](n''l_{\pm 1/2}); l \pm 1/2, m\rangle. \end{aligned}$$

In the wave functions on the right-hand side of Eq. (B2), the two $s_{1/2}$ electrons are first coupled to form a state with angular momentum 1 or 0. This is then coupled with either a $l_{+1/2}$ or $l_{-1/2}$ electron to form the final state with the angular momentum indicated after the semicolon.

The magnetic-dipole interaction energy is given by Eq. (4). The method of evaluating the matrix elements of this interaction is well known.¹⁵

The results for $A(\gamma^2l_{\pm 1/2})$ written in terms of single-electron coupling constants are given below:

$$\begin{aligned} A(\gamma^2l_{+1/2}) &= a(n''l_{+1/2}) \left\{ \alpha_0^2 + \left[\frac{-4l^2+8l-1}{3(2l+1)^2} + \frac{4(2l+3)\xi}{3(2l+2)(2l+1)^2} \right] \alpha_1^2 + \alpha_2^2 \right\} \\ &\quad + a(n''l_{-1/2}) \left\{ \frac{4l(2l-1)}{3(2l+1)^2} \alpha_1^2 \right\} + a(ns) \left\{ \frac{2}{3(2l+1)} \alpha_1^2 - \frac{2\sqrt{3}}{3(2l+1)} \alpha_1 \alpha_2 \right\} \\ &\quad + a(n's) \left\{ \frac{2}{3(2l+1)} \alpha_1^2 + \frac{2\sqrt{3}}{3(2l+1)} \alpha_1 \alpha_2 \right\} + [a(ns)]^{1/2} [a(n's)]^{1/2} \left\{ \frac{2\sqrt{6}}{3(2l+1)} \alpha_0 \alpha_1 \right\}, \quad (\text{B3}) \\ A(\gamma^2l_{-1/2}) &= a(n''l_{+1/2}) \left\{ \left[\frac{2(2l+2)(2l+3)}{3(2l+1)^2} + \frac{4(2l+3)\xi}{3(2l)(2l+1)^2} \right] \alpha_1^2 \right\} \\ &\quad + a(n''l_{-1/2}) \left\{ \alpha_0^2 + \frac{4l^2-5}{3(2l+1)^2} \alpha_1^2 + \alpha_2^2 \right\} + a(ns) \left\{ -\frac{2}{3(2l+1)} \alpha_1^2 + \frac{2\sqrt{3}}{3(2l+1)} \alpha_1 \alpha_2 \right\} \\ &\quad + a(n's) \left\{ -\frac{2}{3(2l+1)} \alpha_1^2 - \frac{2\sqrt{3}}{3(2l+1)} \alpha_1 \alpha_2 \right\} + [a(ns)]^{1/2} [a(n's)]^{1/2} \left\{ -\frac{2\sqrt{6}}{3(2l+1)} \alpha_0 \alpha_1 \right\}. \end{aligned}$$

¹⁴ A. R. Edmonds, *Angular Momentum in Quantum Mechanics* (Princeton University Press, Princeton, New Jersey, 1960).

¹⁵ Reference 14, Chap. 7.

In deriving Eq. (B3) the following relation was used¹⁶:

$$\langle n, \frac{1}{2}, l, l + \frac{1}{2} \| T_e^{(1)} \| n, \frac{1}{2}, l, l - \frac{1}{2} \rangle = - \langle n, \frac{1}{2}, l, l - \frac{1}{2} \| T_e^{(1)} \| n, \frac{1}{2}, l, l + \frac{1}{2} \rangle = - \frac{I \xi}{\mu_I 4} \frac{(2l+1)(2l+3)}{[2l(l+1)(2l+1)]^{1/2}} a(nl_{l+1/2}),$$

where ξ is a relativistic correction factor. If all relativity and nuclear-size corrections are neglected, it follows that (in Koster's notation)

$$A(\gamma^2 l_{l+1/2}) = - \frac{\mu\mu_0}{I(l+\frac{1}{2})} \left\{ - \langle r^{-3} \rangle_{n'l} \frac{4l(l+1)}{2l+3} (\alpha_0^2 + \alpha_2^2) - \left\{ \langle r^{-3} \rangle_{n'l} \frac{4l(3l+5)}{3(2l+3)} + \frac{16\pi}{9} [\psi_{n_s}(0)^2 + \psi_{n'_s}(0)^2] \right\} \alpha_1^2 \right. \\ \left. + \frac{16\sqrt{3}\pi}{9} [\psi_{n_s}(0)^2 - \psi_{n'_s}(0)^2] \alpha_1 \alpha_2 - \frac{16(\sqrt{6})\pi}{9} \psi_{n_s}(0) \psi_{n'_s}(0) \alpha_0 \alpha_1 \right\},$$

$$A(\gamma^2 l_{l-1/2}) = - \frac{\mu\mu_0}{I(l-\frac{1}{2})} \left\{ - \langle r^{-3} \rangle_{n'l} \frac{4l(l+1)}{2l+1} (\alpha_0^2 + \alpha_2^2) - \left\{ \langle r^{-3} \rangle_{n'l} \frac{(3l-2)4(l+1)}{3(2l+1)} - \frac{16\pi}{9} \frac{(2l-1)}{(2l+1)} [\psi_{n_s}(0)^2 + \psi_{n'_s}(0)^2] \right\} \alpha_1^2 \right. \\ \left. - \frac{16\sqrt{3}\pi}{9} \frac{(2l-1)}{(2l+1)} [\psi_{n_s}(0)^2 - \psi_{n'_s}(0)^2] \alpha_1 \alpha_2 + \frac{16(\sqrt{6})\pi}{9} \frac{(2l-1)}{(2l+1)} \psi_{n_s}(0) \psi_{n'_s}(0) \alpha_0 \alpha_1 \right\}.$$

Our wave functions for the excited configuration (i.e., the functions with the α_1 and α_2 coefficients) are the negatives of Koster's. Thus the sign of the $\alpha_0 \alpha_1$ term differs from Koster which means only that we would obtain from the solution of the secular determinant the negative of the values of α_1 and α_2 which Koster calculates. We do disagree with Koster's value for the l electron α_1^2 term in $A(\gamma^2 l_{l-1/2})$. Because of the small size of this term, however, there will be no change in Koster's conclusion.

If we make the approximation that $\alpha_1^2 \ll 1$, which is well justified, then Eq. (B3) can be rewritten

$$A(\gamma^2 l_{l+1/2}) = a(l_{l+1/2}) - a_s, \quad A(\gamma^2 l_{l-1/2}) = a(l_{l-1/2}) + a_s.$$

This result has also been obtained by a somewhat different argument by Eck.¹⁷

¹⁶ A. Lurio, M. Mandel, and R. Novick, Phys. Rev. **126**, 1758 (1962).

¹⁷ T. G. Eck and P. Kusch, Phys. Rev. **106**, 958 (1957).